Comparative Eigenvalue Analysis of Synchronous Machine Emulations and Synchronous Machines

Eneko Unamuno[1*], Jon Are Suul[2,3], Marta Molinas[2] and Jon Andoni Barrena[1]
[1] Electronics and Computing Department, Mondragon Unibertsitatea, Arrasate-Mondragón, Spain
[2] Department of Engineering Cybernetics, Norwegian University of Science and Technology, Trondheim, Norway
[3] SINTEF Energy Research, Trondheim, Norway
*E-mail: eunamuno@mondragon.edu

***Abstract*—This paper presents a comparative eigenvalue analysis of the stability characteristics and small signal dynamics of four different control strategies for Synchronous Machine Emulation (SME) by power electronic converters, considering a Synchronous Machine (SM) as the benchmark system. The four SME techniques are selected to represent the most established general approaches for emulating the inertial characteristics of SMs in the control of power electronic converters. The small-signal stability assessment is based on the analysis of system eigenvalues, including evaluation of participation factors and parametric sensitivities. All the investigated techniques can be tuned to obtain similar inertial dynamics under grid frequency variations, but exhibit differences in other small-signal characteristics due to the distinct control system implementations. Among the analyzed cases, the current-controlled virtual synchronous machine has the highest damping of the most oscillatory mode. However, the study shows that the most oscillatory modes of the other techniques are associated with the *LCL* impedance, and could be further attenuated by active damping techniques.**

***Index Terms*—Inertia Emulation, Frequency Control, Small-Signal Stability, Synchronous Machine Emulation, Swing Equation, Synchronverter, Virtual Synchronous Machine.**

I. Introduction

Increasing penetration of converter-interfaced generation systems in a power system may lead to challenges for the frequency control because power electronic converters do not inherently contribute to the inertia of the power system [1], [2]. To compensate for this emerging problem, power converters can be controlled to support the grid by providing inertial behavior and primary reserve. Therefore, several control strategies for synchronous machine emulation (SME) by grid-connected converters have emerged during the last decade, as for instance reviewed in [3]–[5].

Although the potential benefits of providing virtual inertia properties from power electronic converters are becoming well known, there is a lack of a clear criteria to choose the right implementation for a given application. This is mainly because the implementations reported in the literature have usually been studied separately for specific applications. Although some comparative studies have been recently published, they have mainly been based on internal comparison of various SME techniques under a specific range of operating conditions [6]–[8]. Thus, a comprehensive characterization or mapping of the different SME techniques against a common benchmark, and corresponding comparative results that can be used as a basis for choosing the right implementation for any given application, are not explicitly available in the literature.

As a step towards a generalized comparative evaluation, this paper presents an assessment of the performance and stability characteristics of four identifiable general classes of SMEs: frequency-derivative (df/dt)-based Inertia Emulation (IE), synchronverters (SV), current-controlled virtual synchronous machines (CCVSM) and voltage-controlled virtual synchronous machines (VCVSM). The comparative evaluation is presented with a grid-connected Synchronous Machine (SM) as a general benchmark, whose typical configuration can be observed in Fig. 1(a). As shown in the figure the SM is driven by a turbine, which is in turn controlled by a governor driven by an active power controller (APC). The reactive power controller (RPC) sets the reference for the exciter, which adapts the rotor voltage of the SM. Fig. 1(b), on the other hand, shows the configuration of a three-phase voltage-source converter (VSC) connected to the grid through a passive *LC* filter, and controlled by an SME technique to emulate the behaviour of an SM.

In the following, we first revisit in Section II the basic modeling and control of SMs and review the most relevant characteristics of the four evaluated types of SME strategies. Based on the presented configurations, Section III introduces the procedure for deriving small-signal models in the *dq*-domain, lists the most relevant conditions for these derivations and presents a validation of the derived models as a basis for subsequent analyses. The model validation is obtained by comparing the time-domain response of the linearized small-signal models with the original non-linear systems by simulation of small disturbances. In Section IV, the assessment of the stability of the evaluated systems is carried out by studying their eigenvalues and the corresponding properties, such as their damping, their participation factors and their sensitivity to parameter variations. Finally, Section V concludes with the most important remarks of the research.

II. Background and Overview of SME Techniques

SME control strategies are inspired by the operational characteristics of classical synchronous generators employed to regulate the frequency and voltage of electric grids. Therefore, these techniques are generally designed to emulate the *swing equation* that determines the electromechanical behaviour of

This is the accepted version of an article published in Proceeding 45th Annual Conference of the IEEE Industrial Electronics Society - IECON 2019
http://dx.doi.org/10.1109/IECON.2019.8927826

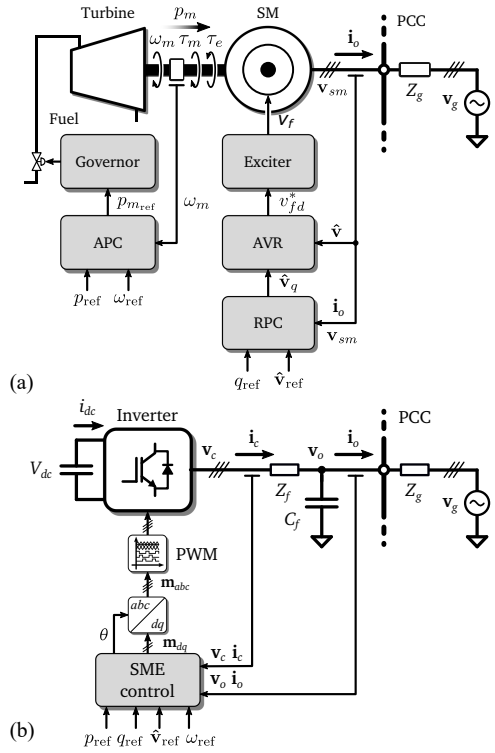

Fig. 1: Configurations of (a) synchronous machine-based generators and (b) power electronic inverter with synchronous machine emulation control

SMs, and to include similar outer loop control functions for the active and reactive power sharing as traditionally applied to SMs. The classical representation of an SM swing equation (in per unit values) is given by [9]:

$$2H\frac{d\omega}{dt} = \tau_m - \tau_e - K_D\Delta\omega \tag{1}$$

where H is the inertia constant of the machine, ω represents the angular speed, and τ_m, τ_e and K_D are the mechanical torque, the electrical torque and the damping factor, respectively. Considering that the variations of the angular speed are usually very small ($\omega \approx 1$ p.u.) , the SM swing equation is usually expressed directly by a power balance instead of the torque balance given by (1). This approximation will be assumed for all the evaluated SME techniques.

According to [3], virtual inertia can be provided from SME controlled converters in two general ways. Either, the inertial characteristics can be obtained by simulating the electromechanical swing equation of a synchronous machine, or the inertial power response that would result from a synchronous machine can be calculated from the estimated grid frequency and its derivative.

In frequency-derivative-based IE techniques, the reference for the inertial power contribution calculated from the frequency derivative can be easily utilized by a conventional control system. However, such techniques will depend on a Phase Locked Loop (PLL) or other similar grid synchronization methods. This implies that they are not inherently applicable in islanded systems without physical inertia [3]. Therefore, IE-controlled converters should be considered as *grid-supporting* devices [10].

SME methods relying on simulation of a virtual swing equation can ensure the same operational flexibility as SMs, which means they operate as *grid-forming* devices. Thus, they are classified in the following as Virtual Synchronous Machines (VSMs). Such VSM-based SME techniques can be implemented in many different ways, and the simulated SM model can be expressed to provide either a current reference or a voltage reference for the control of the power electronic converter [3], [4]. The specific case where a simulated SM model provides a voltage reference used directly for Pulse Width Modulation (PWM) of the converter output voltage is usually labelled as a synchronverter, as introduced in [11], or as a Virtual Synchronous Generator (VSG) when based on the implementation presented in [12]. The other commonly applied approaches for VSM-based control rely on the simulated SM model configured to provide either current references or voltage references for closed loop current or voltage control of the converter, respectively.

On the basis of these considerations, SME techniques can be generally classified in four main groups:

- Inertia-emulation (IE) based on the grid frequency derivative [13]–[15]
- Synchronverter (SV) [11], [16]
- Current-controlled virtual synchronous machine (CCVSM) [6], [7], [17]
- Voltage-controlled virtual synchronous machine (VCVSM) [18]–[20]

Even though we can find several varieties of these techniques in the literature, the aim of this paper is to evaluate the core structure of the most employed controllers. Therefore the analyzed techniques do not include any additional loop for secondary purposes such as current limitation or active damping of resonances. The main characteristics of the techniques studied in this paper and references for the assumed implementations are collected in Tab. I. In addition, Fig. 2 illustrates their detailed control diagrams including the most relevant variable names.

III. Small-Signal Modelling and Validation of SME Control Strategies

Comparison of the SM operation and SME controlled power converters is conducted in two different ways, following a similar methodology for modelling and model validation as in [22]. Firstly, we evaluate the dynamic behaviour by simulation under different disturbances in this section. These simulations serve not only to observe the response of each analyzed system, but also to verify the analytical models by comparison with a non-linear circuit-based simulation model. Subsequently, we will identify the characteristics of each SME implementation in terms of their small-signal dynamics.

A. Small-signal modelling

In order to carry out the small-signal analysis we first derive the state equations that define the dynamics of the analyzed

This is the accepted version of an article published in Proceeding 45th Annual Conference of the IEEE Industrial Electronics Society - IECON 2019
http://dx.doi.org/10.1109/IECON.2019.8927826

TABLE I: Main characteristics of the studied SME techniques

Control technique	Acronym	Main characteristics	References
Inertia-emulation based on the grid frequency derivative	IE	Power reference calculated from an assumed swing equation Output frequency usually estimated by a PLL A frequency droop is included for power sharing purposes Significant low-pass filtering of the frequency usually required because of the derivative term Damping term equivalent to a frequency droop Power references are recalculated into current references by means of the measured voltage	[13], [14]
Synchronverter	SV	Active power control based on a frequency droop and a virtual swing equation Damping term equivalent to a frequency droop Does not include voltage or current regulators, so it cannot inherently limit the current The steady-state frequency is externally fixed for the assumed implementation	[11], [16]
Current-controlled virtual synchronous machine	CCVSM	Active power control based on a frequency droop and a virtual swing equation Damping term based on an estimated frequency Simplified electrical model of a SM in the controller, which provides current references Does not include a PLL for synchronization in the assumed implementation	[7], [17], [21]
Voltage-controlled virtual synchronous machine	VCVSM	Active power control based on a frequency droop and a virtual swing equation Damping term based on the frequency estimated by a PLL Includes a quasi-stationary virtual *RL* impedance Assumed implementation includes a PLL to determine the steady-state output frequency	[19], [20]

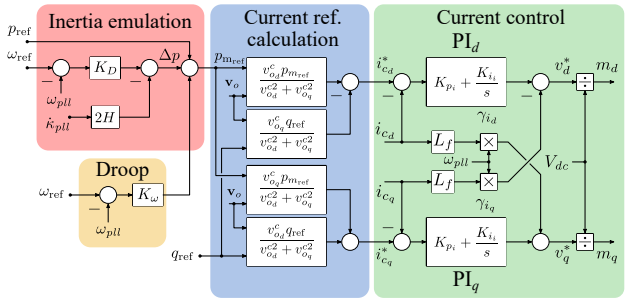

(a) Inertia-emulation

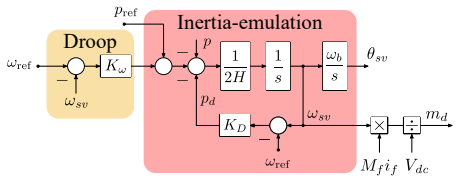

(b) Synchronverter

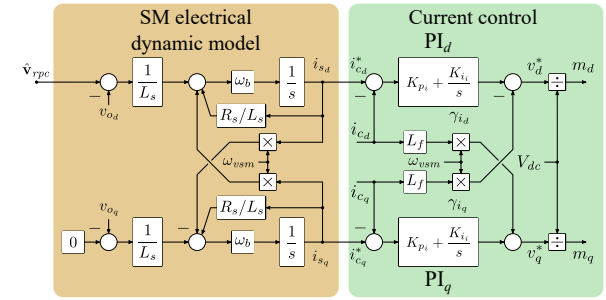

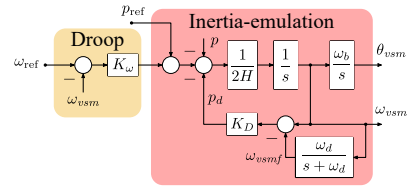

(c) Current-controlled VSM

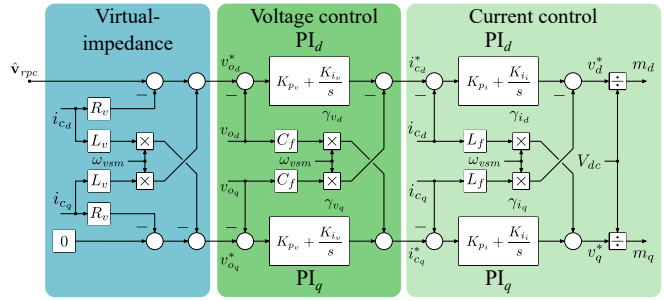

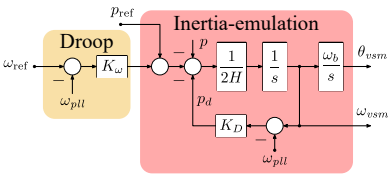

(d) Voltage-controlled VSM

Fig. 2: Studied SME controller structures

system, including physical elements as well as control algorithms. In this paper all the equations employed to model the SM and SME controlled converters are represented in rotating reference frames—i.e. in the *dq* domain—by applying the amplitude-invariant Park transform.

Taking into account that some of the differential equations are non-linear, we solve the system equations for the steady-state operating point resulting from a given set of input signals to obtain the linearization point $\bar{x}$. This equilibrium point of the dynamic system model is computed by setting the derivative terms to zero and solving the resulting set of algebraic equations. We then obtain the small-signal state-space model on the general form of $\dot{\tilde{x}} = \mathbf{A}\tilde{x} + \mathbf{B}\tilde{u}$, linearized at $\bar{x}$, by employing Taylor series expansion, which enables

This is the accepted version of an article published in Proceeding 45th Annual Conference of the IEEE Industrial Electronics Society - IECON 2019
http://dx.doi.org/10.1109/IECON.2019.8927826

the use of linear techniques for stability analyses. The validity and accuracy of the linearized models for representing the dynamics of the investigated configurations in response to small perturbations is confirmed by comparison to the simulated time-domain response of the non-linear circuit-based models used as starting point for the derivation. These simulations also illustrate the dynamic response of the excited modes in each of the investigated cases. For the sake of brevity and readability, and due to space constraints, we do not include the analytical development of the SM and SME controlled converters. The reader is referred to the diagrams illustrated in Fig. 2 and the models presented in [7], [11], [13], [19], [23] for more details about the state-space modelling of the investigated systems.

B. Parameter values and assumed conditions

Most of the parameters employed for the analyses in the following sections are gathered from [7], [19], [23]. However, we have modified some of the parameters to carry out a fair comparative evaluation of their properties. In this sense, we have adjusted the damping term (K_D) and the virtual inertia (H) of the techniques so that their steady-state and transient responses (i.e. the rate of change of the output frequency or RoCoF) under grid frequency perturbations are similar.

The parameters that are shared for the SM-based generator and SME-controlled converters are listed in Table II, as for instance the base values for the per unit calculations or the reference values for the controllers. Similarly, Table III lists the parameter values that are specific to each of the analyzed systems. The results shown in the next sections are obtained considering the following conditions:

1) The reactive power controllers are not considered in the study. They are disabled by setting the reactive power reference q_{ref} and the droop gain K_q to zero.
2) All the analyzed models are linearized at a steady-state point of operation of $p = 0.5$ p.u., while the simulations are started at a different operating condition before a disturbance that will bring the systems back to the linearization point is imposed.
3) The delay resulting from the PWM operation of the converter is modelled as a second order transfer function according to the Padé approximation proposed in [24].
4) The model of the SM is a fifth-order model that takes into account the damper windings of the machine and is obtained from [9], [23].
5) In the case of the IE and VCVSM control the PLL is composed by a classical PI controller that locks to the filter capacitor voltage by regulating its q-axis voltage component, v_{o_q}, to zero.
6) A constant dc-link voltage or an ideal compensation for measured dc voltage in the calculation of the modulation index according to [25] is assumed. Thus, the dynamics of the ac-side are assumed to be effectively decoupled from the dc-side of the converter.
7) For all the cases, the switching frequency is assumed to be 5 kHz.

TABLE II: Parameter values that are common for the analyzed systems connected to ac grids

Parameter	Value	Parameter	Value
S_b	2.75 MVA	P_{ref}	0.5 p.u.
V_b	690 V	Q_{ref}	0 p.u.
ω_b	$2\pi 50$ rad	$\hat{\mathbf{v}}_{\text{ref}}$	1 p.u.
$\mathbf{v}_g$	1 p.u.	Z_g	$0.01 + j0.2$ p.u.
ω_{ref}	1 p.u.	K_ω	20

TABLE III: Parameter values that are specific for each of the analyzed systems connected to ac grids

	SM	IE	SV	CCVSM	VCVSM
L_f	–	0.08 p.u.			
R_f	–	0.03 p.u.			
C_f	–	0.074 p.u.			
L_s	0.05 p.u.	–	–	0.25 p.u.	–
R_s	0.001 p.u.	–	–	0.1 p.u.	–
L_v	–	–	–	–	0.2 p.u.
R_v	–	–	–	–	0
H	1 s	0.025 s	1 s		
K_D	–	2	1	5	5
K_{p_i}	–	0.085	–	0.085	
K_{i_i}	–	4.69	–	4.69	
K_{p_v}	–	–	–	–	0.59
K_{i_v}	–	–	–	–	736
T_s	–	0.1 ms			
T_{ex}	0.1 s	–	–	–	–
T_{gt}	0.5 s	–	–	–	–

C. Model validation and performance evaluation

In order to study the performance of each controller and to ensure the validity of the derived small-signal models for the consequent eigenvalue analysis, we simulate these models against the original non-linear models and compare their behaviour under reference power and grid frequency variations.

1) Active power reference variation: Fig. 3 shows the output power and angular speed of the SM for a 0.1 p.u. variation of the power reference p_{ref}. The curves show that the small-signal state-space model and the original non-linear model coincide for this perturbation, which corroborates that the linearized state-space model is accurately representing the dynamics of the system in the region around the linearization point. The small-signal model of the SM is therefore adequate for the eigenvalue-based stability analysis.

As shown by the results in Fig. 3, the output power of the SM stabilizes to a constant value of 0.5 p.u. after a low-frequency oscillatory transient, which demonstrates that the active power of the machine is correctly controlled to the reference value. It can also be noticed that the rotor speed or equivalent frequency ω has a small oscillation with the same frequency and damping as the oscillations in the power, before it returns to the initial value of 1.0 p.u.

Fig. 4 shows the same curves for the four types of SME control. As can be seen from the figure, all curves show a very good agreement between the non-linear and the developed small-signal models. Moreover, from these results we can conclude that SME controlled converters do not experience

This is the accepted version of an article published in Proceeding 45th Annual Conference of the IEEE Industrial Electronics Society - IECON 2019
http://dx.doi.org/10.1109/IECON.2019.8927826

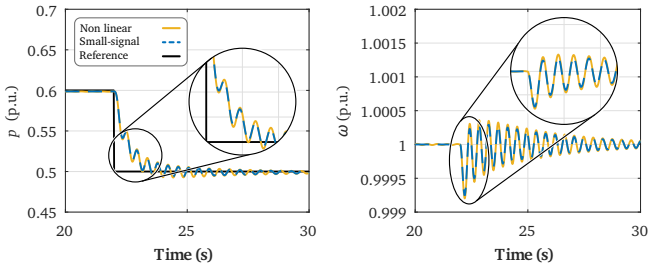

Fig. 3: Dynamic response of a grid-connected SM over a power reference variation: output power in the left and machine frequency in the right

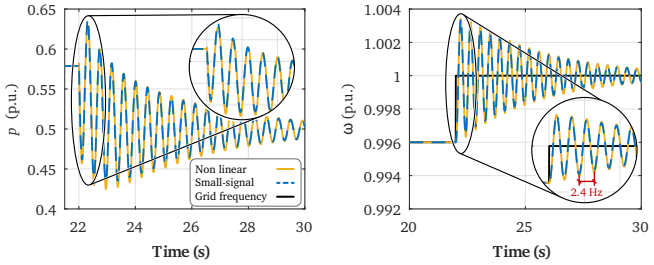

Fig. 5: Dynamic response of a grid-connected SM over a grid frequency variation: output power in the left and machine frequency in the right

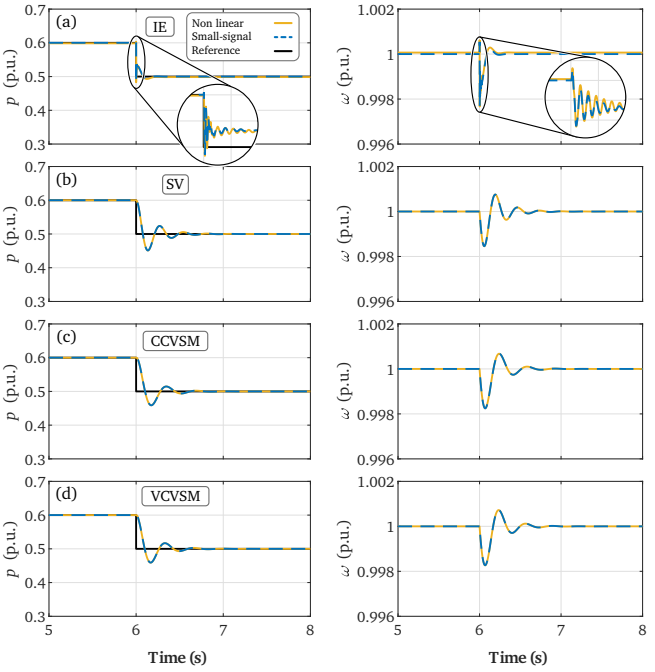

Fig. 4: Dynamic response of grid-connected SME controlled inverters over a power reference variation: output power in the left and controller frequency in the right

the poorly damped low frequency oscillations observed in the SM, and their response over a reference power variation is much smoother in comparison. This is largely because a much higher damping can be selected for the emulation of the *swing equation* in the SME techniques than what is a reasonable equivalent damping of a SM where the parameters are determined by the electromagnetic design. Furthermore, the SME techniques do not depend on a slow governor like the SM.

The SV, CCVSM and VCVSM show a similar behaviour with only minor differences in their overshoot and the time they require to reach the steady-state operation. However, the time response can be adapted by varying the emulated inertia and damping factor of the *swing equation* included in their control strategies.

The IE algorithm has a different transient response compared to the VSM-based SME techniques. In this case, when we apply the power reference step, the IE-controlled VSC suddenly increases its output power. This is also reflected in the frequency of the controller, which in this case corresponds to the frequency of the PLL. This instantaneous variation occurs because of how the *swing equation* is employed in each approach, as explained in previous sections. Therefore, it is important to note that the SV, CCVSM and VCVSM control provide inertial behaviour when the power reference is changed, whereas IE techniques reproduce almost instantaneously—i.e. without inertial behaviour—this variation in the output of the converter.

2) Grid frequency variation: In this case we evaluate the SM and SME controlled converters for a 0.4% grid frequency variation. Fig. 5 shows the dynamic response of the SM-based generator output power and rotor speed for this perturbation. Both curves show a very oscillatory response with an oscillation frequency of approximately 2.4 Hz. These results indicate that the weakly-damped dominant eigenvalues of the system are significantly excited by the grid frequency step, which will be analyzed in detail in the next section.

For the SME-controlled converters, the dynamic response under the same grid frequency variation is shown in Fig. 6. In this case the four control strategies provide a similar inertial behaviour under the frequency perturbation. The SV, CCVSM and VCVSM exhibit a slightly higher overshoot than the IE technique. Apart from that, the four controllers generate a similar rate of change in the output frequency and their steady-state points of operation are very close. Referring back to the parameters defined for the SME techniques in Table III, some of the differences between the four techniques are due to the selection of parameters. Although some parameters have been adapted to obtain a similar dynamic behaviour of the four techniques under grid frequency variations, the different schemes do not inherently provide equal response with the same parameters and an exhaustive analysis of the parameter tuning is beyond the scope of this comparative analysis.

IV. Eigenvalue Analysis of SME Techniques

One of the most classical approaches for small-signal stability assessment is to study the eigenvalues of the state matrix $\mathbf{A}$ of the linearized state-space model. The attributes of these eigenvalues, such as their damping factor, their oscillation frequencies or their sensitivity to parameter variations provide useful information about the dynamic properties of the system

This is the accepted version of an article published in Proceeding 45th Annual Conference of the IEEE Industrial Electronics Society - IECON 2019
http://dx.doi.org/10.1109/IECON.2019.8927826

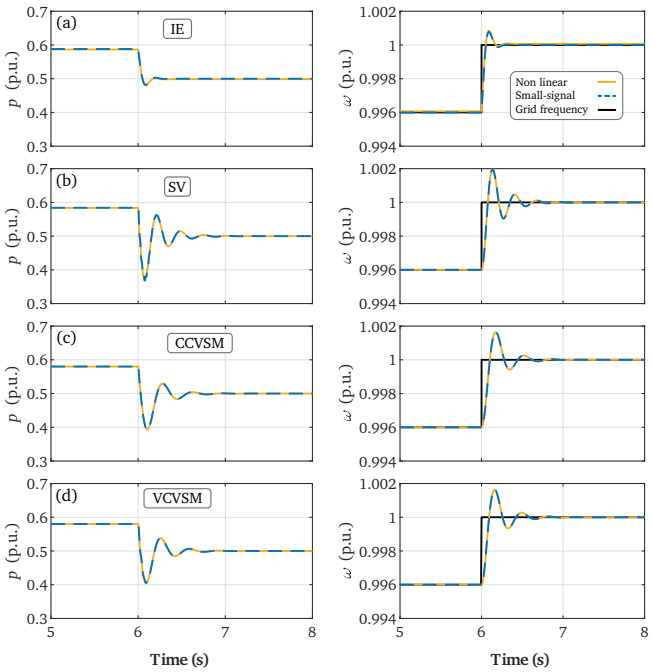

Fig. 6: Dynamic response of grid-connected SME controlled inverters over a grid frequency variation: output power in the left and controller frequency in the right

and facilitate the design/adaptation of controllers to improve these properties [9].

For the investigated operating condition, the numerical values of the eigenvalues for all the studies cases and their most relevant properties are listed in Table IV. The rows highlighted in grey represent the eigenvalues with the lowest damping factors. If excited, these dominant eigenvalues will determine the most poorly damped dynamic behaviour of that system around the linearization point. Although the results in Table IV are obtained for a single operation point, results from studies of individual cases in previous literature indicate that the general characteristics will still be valid for a reasonable range of combinations of controller and/or physical parameters [7], [19], [20], [23]. Taking that into account, and due to space constraints, the results are limited to a single set of parameters.

Apart from the damping factors and the frequencies of the eigenvalues, we have also calculated the sensitivity of the eigenvalue locations in the imaginary plane with respect to the parameters of the system (ρ_k). This information is useful to identify which parameters are related to instabilities or poorly damped oscillations, and could be modified to improve the stability margins. In this case, we have evaluated the normalized parametric sensitivity as in [7]

The results from Table IV show that all the eigenvalues of the systems have a negative real part. This corroborates the conclusions from the time-domain simulations, where all the analyzed systems were shown to be stable. From these values we can also see that, apart from the CCVSM, the rest of systems contain some eigenvalue with a low or very low damping factor. This implies that even if all the systems

TABLE IV: Eigenvalue analysis of the SM and SME-controlled converters

Case	i	Eigenvalue λ_i	Damp. ζ_i	Freq. f_i (Hz)	Param. Sen. $\sigma_{i_{\max}}$
SM	1 : 10	-0.19	1	-	$K_{i_{ex}}$, L_l, L_{m_d}
		-1.86	1	-	T_{gt}, L_{m_d}, L_{m_q}
		-5.83	1	-	L_{m_d}, L_{m_q}, $R_{k_{q1}}$
		$-4.98 \pm j3.39$	0.83	0.54	T_{ex}, L_{m_d}, L_{m_q}
		$-0.28 \pm j14.89$	0.02	2.37	L_l, L_{m_d}, L_{m_q}
		-32.85	1	-	L_{m_d}, R_{k_d}, L_{f1_d}
		$-9.87 \pm j314.08$	0.03	49.99	R_g, L_{m_d}, L_{f1_d}
IE	1 : 14	$-11.2 \pm j0.59$	1	0.09	K_{i_c}, K_{p_i}, T_s
		$-16.27 \pm j27.86$	0.5	4.43	$K_{i_{\text{PLL}}}$, $K_{p_{\text{PLL}}}$, K_ω
		-1689.04	1	-	K_{p_i}, L_g, L_f
		$-157.13 \pm j2227.21$	0.07	354.47	K_{p_i}, C_f, $K_{p_{\text{PLL}}}$
		-6238.67	1	-	K_{p_i}, T_s, L_f
		$-1121.42 \pm j7210.9$	0.15	1147.65	T_s, L_f, C_f
		$-2213.96 \pm j8809.25$	0.24	1402.04	T_s, L_f, K_{p_i}
		-31821.78	1	-	T_s, K_{p_i}, L_f
		-33292.45	1	-	T_s, K_{p_i}, L_f
SV	1 : 13	$-20000 \pm j0$	1	-	T_s
		-0.02	1	-	K, L_g, L_f,
		$-5.3 \pm j23.25$	0.22	3.7	H, K_ω, K_D
		$-14.58 \pm j314.16$	0.046	50	R_g, L_g, L_f
		$-20000.11 \pm j59.14$	1	9.41	T_s, H, L_f
		$-6.37 \pm j4517.06$	0.0014	718.91	R_f, L_f, L_g
		$-6.38 \pm j5145.35$	0.0012	818.91	R_f, L_f, L_g
CCVSM	1 : 18	-5.2	1	-	ω_d, K_D, L_s
		-9.73	1	-	K_{i_c}, K_{p_i}, L_s
		-11.79	1	-	K_{p_i}, K_{i_c}, L_s
		$-5.54 \pm j18.34$	0.29	2.92	H, K_ω, K_D
		-36.2	1	-	K_{i_c}, K_{p_i}, L_s
		$-73.27 \pm j308.52$	0.23	49.10	R_s, L_s, L_g
		$-1578.44 \pm j3101.65$	0.45	493.64	K_{p_i}, C_f, L_f
		$-1313.05 \pm j3804.04$	0.33	605.43	K_{p_i}, C_f, L_s
		$-2107.2 \pm j6855.36$	0.29	1091.06	T_s, L_f, C_f
		$-2408.36 \pm j7477.7$	0.31	1190.11	T_s, L_f, C_f
		$-32644.58 \pm j312.57$	1	49.75	T_s, K_{p_i}, L_f
VCVSM	1 : 18	$-5.44 \pm j19.09$	0.27	3.04	H, K_ω, L_v
		-11.26	1	-	K_{p_i}, K_{i_c}, K_{i_v}
		-11.34	1	-	K_{p_i}, K_{i_c}, T_s
		$-14.16 \pm j35.61$	0.37	5.67	$K_{p_{\text{PLL}}}$, H, K_D
		$-29.51 \pm j196.87$	0.15	31.32	K_{p_v}, K_{i_v}, L_v
		$-2122.76 \pm j550.59$	0.97	87.63	K_{p_i}, K_{p_v}, L_g
		$-4934.58 \pm j1131.71$	0.98	180.12	K_{p_i}, T_s, L_f
		$-663.77 \pm j6912.45$	0.096	1100.15	T_s, C_f, K_{p_v}
		$-104.64 \pm j7812.09$	0.013	1243.33	T_s, C_f, K_{p_v}
		$-32160.9 \pm j426.17$	1	67.83	T_s, K_{p_i}, L_f

Less-damped modes
Modes associated to the inertial response

are stable, they contain modes that can cause poorly damped oscillations.

In the case of the SM, the results show that the oscillation frequency of 2.37 Hz of the dominant eigenvalues ($\lambda_{6,7}$) corresponds to the frequency of the oscillation identified in Fig. 5. In fact, the parametric sensitivity shows that these eigenvalues are mainly influenced by the physical inductances L_l, L_{m_d} and L_{m_q} of the machine, meaning that the stability margins of this system are primarily determined by the design of the machine itself. From Table IV, we can also notice that the SM has a pair of poorly damped eigenvalues at a frequency of nearly 50 Hz. According to previous studies, this oscillation mode is usually neglected for SMs because of the slow mechanical reaction of the machine [26]. However, such "synchronous

This is the accepted version of an article published in Proceeding 45th Annual Conference of the IEEE Industrial Electronics Society - IECON 2019
http://dx.doi.org/10.1109/IECON.2019.8927826

frequency resonances" can be also observed in the case of the SV and the CCVSM, and due to the fast regulation capabilities of power converters they might cause power oscillations and should be damped by adapting the controllers as discussed in [7], [26]. In the case of the SV, these modes have a relatively low damping factor, and can significantly influence the dynamic response to certain perturbations. In the case of the CCVSM these oscillation modes are dominant—they have the lowest damping factor—but they can be effectively damped by the virtual resistance (R_s) [7]. At this point it should be highlighted that unlike the SV and the CCVSM, the IE- and VCVSM-controlled converters do not exhibit these "synchronous frequency resonances".

The most critical eigenvalues of the VCVSM- and IE-controlled systems are affected mainly by the filter capacitor C_f and the controller proportional gains $K_{p_{\mathrm{PLL}}}$, K_{p_i} and K_{p_v}, associated with the PLL, the current control and voltage control loops, respectively. Regarding the SV and the CCVSM, from Table IV we can deduce that their dominant eigenvalues are primarily affected by the grid-side inductance L_g as well as the filter inductance with its parasitic resistance (L_f and R_f) in the case of the SV and the virtual machine windings (L_s and R_s) in the case of the CCVSM. This means that the stability margins of the SV are mainly determined by the parameters of the electrical circuit whereas the CCVSM is more influenced by the control parameters.

From Table IV we can also identify the modes that are related to the inertial behaviour of SME-controlled inverters (highlighted in red), which determine the inertial response of the system. In the case of the SV, the CCVSM and the VCVSM technique we can see that these modes have a very low oscillation frequency ($f_{6,7} = 3.7$ Hz, $f_{7,8} = 2.92$ Hz and $f_{5,6} = 5.67$ Hz, respectively). Regarding the IE technique, the damping term (K_D) and the virtual inertia (H) do not significantly influence any of the modes of the system. However, we can see from the results that the gains of the PLL, from which the inertia is emulated, have a strong influence in two modes with a low oscillation frequency ($f_{2,3} = 4.43$ Hz). From this analysis we can conclude that all the SME techniques have low frequency modes directly or indirectly associated with the emulation of inertial behaviour of the virtual swing equation. In fact, the frequency and power perturbations carried out in Section III cause low frequency oscillations that are directly related to these dynamic modes, meaning that for these perturbations the most influential modes are the ones associated to the emulation of inertia. Although the discussions above are based on the eigenvalues at a particular point of operation (0.5 p.u.), the eigenvalue trajectories in Figure 7 show that, except in the IE case, changes in the operation point do not significantly influence the modes of the system. The conclusions from the paper can be hence extrapolated to the entire range of operation. Due to the lack of space, a more in depth analysis of the IE controller is left for future research.

As a means to gain more information about the relation between the states of the system and the eigenvalues, we have also carried out a participation factor analysis according to [9].

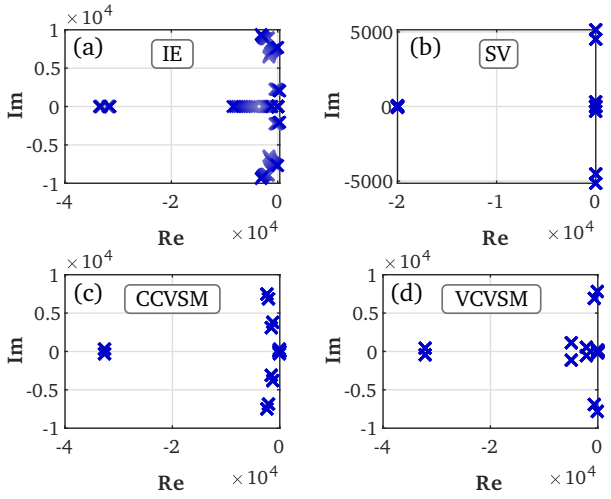

Fig. 7: Location of eigenvalues for different operation points: output power from 0 p.u. (light blue) to 1 p.u. (dark blue)

In order to represent this relationship in a percentage scale, we have also weighted the participation factors as in [27]. In Fig. 8 we show the states that have a weighted participation in the critical mode that is higher than a 10%. These charts show that in most cases the output current of the converter ($\tilde{\mathbf{i}}_c$), the grid-side current ($\tilde{\mathbf{i}}_o$) and the filter capacitor voltage ($\tilde{\mathbf{v}}_o$) are the states with a highest participation factor. The CCVSM is the only exception as the most influencing state is the current flowing through the virtual SM windings ($\tilde{\mathbf{i}}_s$), but the grid-side currents also have a high participation factor in this case. In the case of the IE- and the VCVSM-controlled inverter we can also see that the states associated with the delay of the PWM ($\tilde{\boldsymbol{\beta}}_2$) have a significant influence in the dominant eigenvalues.

Based on the study of the eigenvalues and their properties, the CCVSM provides the highest stability margins among the studied approaches. However, the oscillation frequencies of the critical modes for the other VSM-based cases, i.e. the SV and the VCVSM, are near the resonance frequency of the *LCL* impedance between the converter and the grid. Thus, it can be expected that utilization of active damping techniques for this frequency range might significantly improve the margins of these cases. This consideration is also in accordance with the results obtained in [8].

V. Conclusion

This paper has presented a comparative eigenvalue-based evaluation of four different synchronous machine emulation (SME) techniques in terms small-signal dynamics, taking a synchronous machine (SM) as the benchmark system. The four SME techniques are selected to represent the main general classes of implementations established in literature, and the results show how all these control schemes can provide an inertial response with higher damping than the SM. This is mainly because the SME techniques can be implemented with a higher damping coefficient in the emulated swing equation than what results from the practical design of a SM, but also because the SME techniques can be designed without

This is the accepted version of an article published in Proceeding 45th Annual Conference of the IEEE Industrial Electronics Society - IECON 2019
http://dx.doi.org/10.1109/IECON.2019.8927826

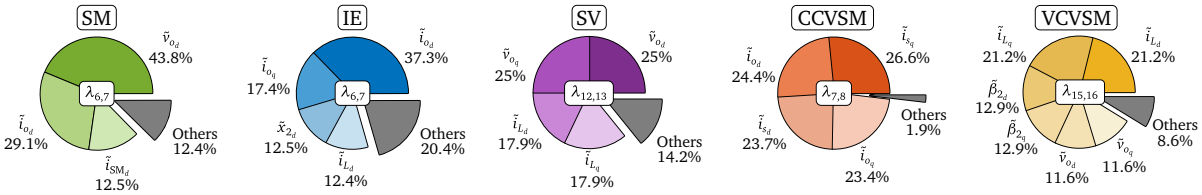

Fig. 8: Participation factors of the most critical eigenvalues

the slow response of a mechanical governor. Among the four investigated SME techniques, the SV, CCVSM and VCVSM provide a similar inertial response under perturbations in the grid frequency as well as in the power reference. While the IE can provide inertial response to frequency variations, it does not exhibit similar dynamics as the other techniques when exposed to power reference variations, since it does not explicitly emulate a SM swing equation and only responds to the variations in the estimated grid frequency.

The eigenvalue analysis has also shown that the CCVSM has the highest stability margins for the investigated operating conditions. However, the eigenvalues of the SV and the VCVSM with the lowest damping are mainly associated with the *LCL* filter dynamics. Thus, active damping techniques designed for attenuating *LC*-oscillations can significantly improve the stability margins of these control techniques. Thus, it is expected that all the schemes can be designed to ensure sufficient stability margins, but with slightly different small-signal dynamics due to the different control system configurations.

Acknowledgment

This work has been partially funded by the ERDF/Ministry of Science, Innovation and Universities—State Research Agency/MTM2017-82996-C2-2-R and by the Basque Government under the project Road2DC (KK–2018/00083).

References

[1] J. O'Sullivan, P. S. A. M. A. Rogers, D. Flynn, and M. O'Malley, "Studying the maximum instantaneous non-synchronous generation in an island system–frequency stability challenges in ireland," *IEEE Transactions on Power Systems*, vol. 29, no. 6, pp. 2943–2951, 2014.

[2] T. B. A. Ulbig and G. Andersson, "Impact of low rotational inertia on power system stability and operation," *IFAC Proceedings Volumes*, vol. 47, no. 3, pp. 7290–7297, 2014.

[3] S. D'Arco and J. A. Suul, "Virtual synchronous machines—Classification of implementations and analysis of equivalence to droop controllers for microgrids," in *2013 IEEE Grenoble PowerTech Conf.*, jun 2013, pp. 1–7.

[4] H. Alrajhi Alsiraji and R. El-Shatshat, "Comprehensive assessment of virtual synchronous machine based voltage source converter controllers," *IET Gener. Transm. Distrib.*, vol. 11, no. 7, pp. 1762–1769, may 2017.

[5] H. Bevrani, T. Ise, and Y. Miura, "Virtual synchronous generators: A survey and new perspectives," *Int. J. Electr. Power Energy Syst.*, vol. 54, pp. 244–254, jan 2014.

[6] Y. Chen, R. Hesse, D. Turschner, and H.-p. Beck, "Comparison of methods for implementing virtual synchronous machine on inverters," in *Int. Conf. Renew. Energies Power Qual.*, 2012, pp. 1–6.

[7] O. Mo, S. D'Arco, and J. A. Suul, "Evaluation of Virtual Synchronous Machines with Dynamic or Quasi-stationary Machine Models," *IEEE Trans. Ind. Electron.*, vol. 0046, no. c, pp. 1–1, 2016.

[8] J. A. Suul and S. D'Arco, "Comparative Analysis of Small-Signal Dynamics in Virtual Synchronous Machines and Frequency-Derivative-Based Inertia Emulation," in *2018 IEEE 18th Int. Power Electron. Motion Control Conf.*, no. 268053. IEEE, aug 2018, pp. 344–351.

[9] P. Kundur, *Power System Stability And Control*. New York: McGraw-Hill Education (India) Pvt Limited, 1994.

[10] F. B. J. Rocabert, A. Luna and P. Rodriguez, "Control of power converters in ac microgrids," *IEEE transactions on power electronics*, vol. 27, no. 11, pp. 4734–4749, 2012.

[11] Q.-C. Zhong and G. Weiss, "Synchronverters: Inverters That Mimic Synchronous Generators," *IEEE Trans. Ind. Electron.*, vol. 58, no. 4, pp. 1259–1267, apr 2011.

[12] K. Sakimoto, Y. Miura, and T. Ise, "Stabilization of a power system with a distributed generator by a virtual synchronous generator function," in *2011 IEEE 8th International Conference on Power Electronics and ECCE Asia, ICPE & ECCE 2011*. IEEE, 2011, pp. 1498–1505.

[13] V. Karapanos, S. W. H. De Haan, and K. H. Zwetsloot, "Testing a Virtual Synchronous Generator in a Real Time Simulated Power System," *Int. Conf. Power Syst. Transients*, vol. 31, no. 0, 2011.

[14] M. P. N. van Wesenbeeck, S. W. H. de Haan, P. Varela, and K. Visscher, "Grid tied converter with virtual kinetic storage," in *2009 IEEE Bucharest PowerTech Innov. Ideas Towar. Electr. Grid Futur.*, no. 1. IEEE, jun 2009, pp. 1–7.

[15] D. Duckwitz and B. Fischer, "Modeling and Design of df/dt-based Inertia Control for Power Converters," *IEEE J. Emerg. Sel. Top. Power Electron.*, vol. PP, no. 99, pp. 1–1, 2017.

[16] Q.-C. Zhong and G. Weiss, "Static synchronous generators for distributed generation and renewable energy," in *2009 IEEE/PES Power Syst. Conf. Expo. PSCE 2009*. IEEE, mar 2009, pp. 1–6.

[17] R. Hesse, D. Turschner, and H.-P. Beck, "Micro grid stabilization using the Virtual Synchronous Machine (VISMA)," *2009 Int. Conf. Renew. Energies Power Qual.*, 2009.

[18] D. Chen, Y. Xu, and A. Q. Huang, "Integration of DC Microgrids as Virtual Synchronous Machines into the AC Grid," *IEEE Trans. Ind. Electron.*, vol. 0046, no. c, pp. 1–1, 2017.

[19] S. D'Arco, J. A. Suul, and O. B. Fosso, "A Virtual Synchronous Machine implementation for distributed control of power converters in SmartGrids," *Electr. Power Syst. Res.*, vol. 122, pp. 180–197, 2015.

[20] ——, "Control system tuning and stability analysis of Virtual Synchronous Machines," in *2013 IEEE Energy Convers. Congr. Expo.*, no. September 2013. IEEE, sep 2013, pp. 2664–2671.

[21] H.-P. Beck and R. Hesse, "Virtual synchronous machine," in *2007 9th Int. Conf. Electr. Power Qual. Util.* IEEE, oct 2007, pp. 1–6.

[22] E. Unamuno, A. Rygg, M. Amin, M. Molinas, and J. A. Barrena, "Impedance-Based Stability Evaluation of Virtual Synchronous Machine Implementations in Converter Controllers," in *2018 Int. Power Electron. Conf. (IPEC-Niigata 2018 -ECCE Asia)*. IEEE, may 2018, pp. 759–766.

[23] O. Saborío, "Small-signal modelling and stability analysis of a traditional generation unit and a virtual synchronous machine in grid-connected operation," Master's thesis, NTNU, 2015.

[24] J. L. Agorreta, M. Borrega, J. López, and L. Marroyo, "Modeling and Control of N-Paralleled Grid-Connected Inverters With LCL Filter Coupled Due to Grid Impedance in PV Plants," *IEEE Trans. Power Electron.*, vol. 26, no. 3, pp. 770–785, mar 2011.

[25] C. A. H.-A. N. Kroutikova and T. C. Green, "State-space model of grid-connected inverters under current control mode," *IET Electric Power Applications*, vol. 1, no. 3, pp. 329–338, 2007.

[26] J. Wang, Y. Wang, Y. Gu, W. Li, and X. He, "Synchronous frequency resonance of virtual synchronous generators and damping control," in *2015 9th International Conference on Power Electronics and ECCE Asia (ICPE-ECCE Asia)*. IEEE, jun 2015, pp. 1011–1016.

[27] F. Shahnia and A. Arefi, "Eigenanalysis-based small signal stability of the system of coupled sustainable microgrids," *Int. J. Electr. Power Energy Syst.*, vol. 91, pp. 42–60, 2017.

This is the accepted version of an article published in Proceeding 45th Annual Conference of the IEEE Industrial Electronics Society - IECON 2019
http://dx.doi.org/10.1109/IECON.2019.8927826